Self-Assembling Peptide as a Potential Carrier for Hydrophobic Anticancer Drug Ellipticine: Complexation, Release and In Vitro Delivery

ARTICLE *in* ADVANCED FUNCTIONAL MATERIALS · JANUARY 2009

Impact Factor: 11.81 · DOI: 10.1002/adfm.200800860

7 AUTHORS, INCLUDING:

Shan-Yu Fung
University of British Columbia - Vancouver
31 PUBLICATIONS **620** CITATIONS

SEE PROFILE

Hong Yang
University of British Columbia - Vancouver
26 PUBLICATIONS **517** CITATIONS

SEE PROFILE

FULL PAPER

Self-Assembling Peptide as a Potential Carrier for Hydrophobic Anticancer Drug Ellipticine: Complexation, Release and In Vitro Delivery

By *Shan Yu Fung, Hong Yang, Priya T. Bhola, Parisa Sadatmousavi, Edward Muzar, Mingyao Liu,* and *P. Chen**

The self-assembling peptide EAK16-II is capable of stabilizing hydrophobic compounds to form microcrystal suspensions in aqueous solution. Here, the ability of this peptide to stabilize the hydrophobic anticancer agent ellipticine is investigated. The formation of peptide-ellipticine suspensions is monitored with time until equilibrium is reached. The equilibration time is found to be dependent on the peptide concentration. When the peptide concentration is close to its critical aggregation concentration, the equilibration time is minimal at 5 h. With different combinations of EAK16-II and ellipticine concentrations, two molecular states (protonated or cyrstalline) of ellipticine could be stabilized. These different states of ellipticine significantly affect the release kinetics of ellipticine from the peptide-ellipticine complex into the egg phosphatidylcholine vesicles, which are used to mimic cell membranes. The transfer rate of protonated ellipticine from the complex to the vesicles is much faster than that of crystalline ellipticine. This observation may also be related to the size of the resulting complexes as revealed from the scanning electron micrographs. In addition, the complexes with protonated ellipticine are found to have a better anticancer activity against two cancer cell lines, A549 and MCF-7. This work forms the basis for studies of the peptide-ellipticine suspensions in vitro and in vivo leading to future development of self-assembling peptide-based delivery of hydrophobic anticancer drugs.

1. Introduction

The slow progress in treating severe diseases such as cancer has suggested a growing need for novel approaches to the effective delivery of therapeutics to physiological targets. Drug delivery systems are essential to control pharmacokinetics, non-specific toxicity, immunogenecity, biorecognition, and drug efficacy.[1] In order to develop novel drug delivery systems for clinical use, the design and/or discovery of effective delivery vehicles play an important role. The ideal delivery vehicle should have the following properties: biocompatible, biodegradable, suitable size, high loading capacity, extended circulation time, and capable of accumulating at required pathological sites in the body.[2]

Peptides have shown much potential for drug delivery. The most attractive aspect of peptide-mediated drug delivery is the natural propensities of many peptides for cell penetration and targeting.[3–5] As a result, many novel delivery systems involve peptides to achieve targeted delivery[5–8] for anticancer therapeutics and to cross the cell membrane barrier[9–12] for gene/siRNA delivery. Peptide-based delivery systems have also shown the potential to deliver therapeutic proteins, bioactive peptides, small molecules and nucleic acids.[3,13,14]

A special class of self-assembling, ionic-complementary peptides[15] could be a new and promising biomaterial for constructing drug delivery nanocarriers. The unique amphiphilic structure and the ability of self-assembly of these peptides allow them to encapsulate both hydrophobic chemotherapeutics and hydrophilic protein and oligonucleotides.[15–17] Moreover, no detectable immune response was observed when these peptides were introduced into animals.[18–20] These peptides can spontaneously organize themselves into nano/micro structures that may provide a protected and stable environment for the therapeutic molecules, and facilitate passive targeting.[6] An additional advantage of using such peptide-based carriers is the ease of sequence modification and design to incorporate peptide cell penetration and active targeting capabilities.

[*] Prof. P. Chen, S. Y. Fung, H. Yang, P. Sadatmousavi
Department of Chemical Engineering, University of Waterloo
Waterloo, Ontario N2L 3G1 (Canada)
E-mail: p4chen@cape.uwaterloo.ca
P. T. Bhola
Department of Medical Biophysics, University of Toronto
Toronto, Ontario M5G 1L7 (Canada)
E. Muzar
Department of Materials Science and Engineering
University of Toronto
Toronto, Ontario M5S 3E4 (Canada)
Dr. M. Liu
Latner Thoracic Surgery Research Laboratories
University Health Network Toronto General Research Institute
Toronto, Ontario, M5G 1L7 (Canada)

DOI: 10.1002/adfm.200800860

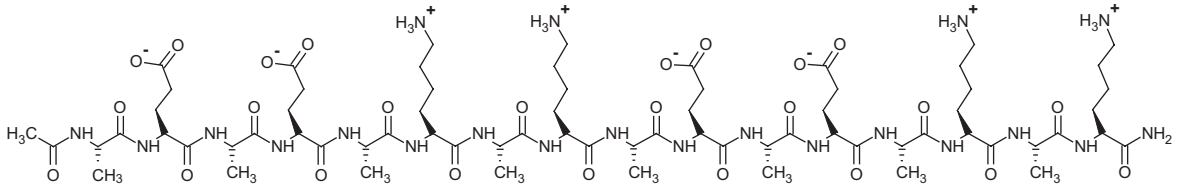

Figure 1. Molecular structure of EAK16-II: AEAEAKAKAEAEAKAK; A is alanine, E glutamic acid and K lysine.

A typical self-assembling, ionic-complementary peptide, EAK16-II (Fig. 1), has been shown to encapsulate hydrophobic compounds readily and stabilize them in aqueous solution. Recent work using pyrene as a model hydrophobic compound demonstrated the promising potential of this peptide in the delivery of hydrophobic anticancer drugs.[21,22] EAK16-II was shown to stabilize pyrene microcrystals in aqueous solution at a concentration ten-thousand fold beyond its solubility in water, indicating a very high loading efficiency. The encapsulated pyrene can be released from the peptide coatings into liposomes and the release rate can be controlled by changing the peptide-to-pyrene ratio during the encapsulation.[21] More recently, this peptide has been used to stabilize microcrystals of the anticancer agent ellipticine in aqueous solution.[22] The stabilized ellipticine microcrystals can have a concentration several hundred times more than its solubility.

Ellipticine is selected as the model hydrophobic anticancer drug in our studies for the following reasons: first, the fluorescence property of ellipticine enables us to monitor the interaction of ellipticine with the peptide and locate it in different micro-environments.[23] Second, ellipticine is extremely hydrophobic, with a low water solubility of ~0.62 μM at neutral pH,[24] which is comparable with that of the model hydrophobic compound pyrene.[25] Third, its great anticancer activity makes ellipticine one of the promising candidates in cancer chemotherapy.[26] Fourth, the discovery of severe side effects of ellipticine derivatives during clinical trials suggests that a novel delivery system is required.[26,27]

In this study, we investigate the effect of peptide and ellipticine concentration on the formation of peptide-ellipticine complexes in aqueous solution over time. This will elucidate of the kinetics of the complex formation in relation to peptide self-assembly. A new methodology developed in our recent work[21] is applied to study the release kinetics of ellipticine from the peptide-ellipticine complexes to egg phosphatidylcholine (EPC) vesicles as cell membrane mimics. The fluorescence technique is the primary tool to characterize the complex formation and the release kinetics, where the change of ellipticine fluorescence is monitored over time. Scanning electron microscopy (SEM) is applied to characterize the dimensions of the peptide-ellipticine complexes. The complexes with various peptide-to-ellipticine ratios (by mass) are further tested on their cellular toxicity against two cancer cell lines, A549 and MCF-7. The cells are treated for different time periods (4–48 h) to reveal the time-dependent toxicity of the complexes. This work will provide comprehensive knowledge on the formation of peptide-ellipticine suspensions, ellipticine release kinetics and cellular toxicity of the complexes, paving the way for future animal studies in the development of self-assembling peptide-based delivery of hydrophobic anticancer drugs.

2. Results and Discussion

The self-assembling peptide EAK16-II has shown the capability of stabilizing a hydrophobic compound and the anticancer agent ellipticine in aqueous solution from our previous studies.[22] Here we report the details of the complexation between EAK16-II and ellipticine, concentration effects on the complex formation, the release kinetics of ellipticine from the complexes to the liposomes and the cellular toxicity of the complexes.

2.1. Time Dependence of the Formation of Peptide-Ellipticine Complexes

To investigate the details of the complexation kinetics, the change in the ellipticine fluorescence of the peptide-ellipticine dispersions was monitored over time. It has been found that ellipticine fluorescence strongly depends on its molecular states and the surrounding environments.[22,23] There are three different molecular states of ellipticine: neutral, crystalline and protonated, with corresponding emission fluorescence peaks at ~390–440 nm, ~468 nm and ~520 nm, respectively. Figure 2a shows the fluorescence spectra of the complex suspension (1.0 mg mL^{-1} ellipticine and 0.2 mg mL^{-1} EAK16-II) at different times. Initially, the fluorescence spectrum exhibits a characteristic of protonated ellipticine with a peak located around 520 nm after 0.5 h stirring. This peak rises with time and reaches a maximum after 6 h; it then decreases with time. Meanwhile, a shoulder located at ~468 nm (crystalline ellipticine) becomes pronounced with time and eventually forms a peak after 9 h. Note that there was no trace of fluorescence from ellipticine crystals (at 468 nm) initially; although ellipticine was in crystalline form when just mixed with the peptide solution, the ellipticine crystals were large, unable to suspend in solution, and thus precipitated at the bottom of the sample vial, not contributing to the fluorescence signal detected.

The intensity changes of the two peaks at 468 and 520 nm were plotted with time in Figure 2b. It can be clearly seen that the intensity at 520 nm increases for the first 6 h to a maximum and then decreases to the initial level after 10 h. On the other hand, the intensity at 468 nm increases with time and reaches a plateau after ~15 h. The latter indicates that ellipticine crystals or microcrystals are gradually stabilized in aqueous solution, to form a peptide-ellipticine suspension with time. The final state of stabilized ellipticine is in crystalline form and equilibrium is reached after ~15 h (considering both I_{468} and I_{520} reaching equilibrium).

The change in the fluorescence of protonated ellipticine with such a trend may indicate a special mechanism of the complex formation. It is speculated that the fresh peptide solution could

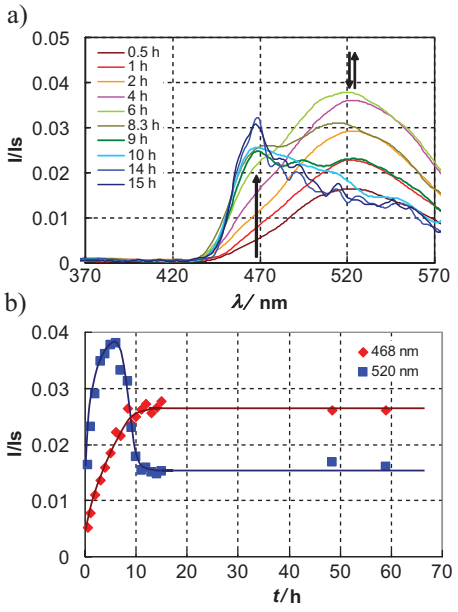

Figure 2. The ellipticine fluorescence from the peptide-ellipticine suspension over time. a) Fluorescence spectra of ellipticine as a function of time; b) the normalized fluorescence intensities at 468 nm (diamonds) and 520 nm (squares) as a function of time. The ellipticine concentration is 1.0 mg mL^{-1} and the peptide concentration is 0.2 mg mL^{-1}.

facilitate the formation of protonated ellipticine. Since ellipticine has a p*K*a of ~6 (pyridine-like nitrogen), it can be protonated in a weak acidic environment.[26,28,29] A fresh EAK16-II (0.2 mg mL^{-1}) in pure water has a pH value of ~4.6, which can cause the protonation of ellipticine. In addition, the peptide molecules consisting of negatively charged glutamic acid residues may help stabilize the protonated ellipticine upon interaction. A similar phenomenon has been reported, in that highly negatively charged sodium dodecyl sulfate (SDS) micelles was found to stabilize protonated ellipticine in pure water.[23,28] The amount of protonated ellipticine increases during the first several hours to a maximum and then disappears when the equilibrium is established. The diminishing of the protonated ellipticine prior to equilibrium may be related to the peptide self-assembly over time and its associated events. As shown in Figure 3, a 0.2 mg mL^{-1} EAK16-II solution can significantly increase the scattered light intensity 30 h after preparation, which is 6 fold higher than that of the fresh peptide solution. This is the evidence of peptide assembly over time under constant mechanical stirring. The formation of EAK16-II assemblies may consume the negatively charged glutamic acid residues as they are complementary to the lysine residues in the assemblies. This in turn reduces the amount of free glutamic acid residues that are able to stabilize the protonated ellipticine. Meanwhile, the pH of the EAK16-II solution was found to increase from ~4.6 (fresh) to 6.4 (30 h after preparation), which is slightly above the p*K*a of ellipticine. The combination of these two effects can induce deprotonation of ellipticine, thereby explaining the disappearance of protonated ellipticine over time.

On the other hand, the peptide assembly does not likely inhibit the formation of stable ellipticine microcrystals. In fact, these peptide assemblies are mainly made of β-sheets, which are

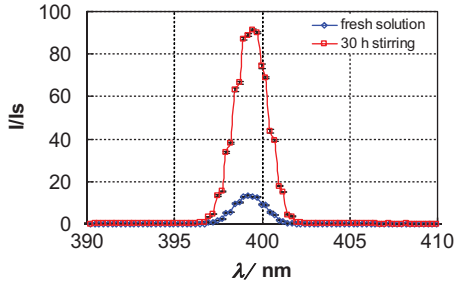

Figure 3. Static light scattering of 0.2 mg mL^{-1} EAK16-II solution at 400 nm before (blue) and after mechanical stirring for 30 h (red).

amphiphilic with hydrophobic and hydrophilic regions on the opposite sides.[30,31] The hydrophobic region can still interact with hydrophobic ellipticine microcrystals to form stable peptide-ellipticine suspensions. It has been shown that EAK16-II can adsorb on hydrophobic surfaces and assemble into stable β-sheet rich nanostructures.[22,31]

2.2. Concentration Effect on the Complex Formation

Figure 4 shows the peptide concentration effect on the formation of peptide-ellipticine complexes at a fixed ellipticine concentration of 1.0 mg mL^{-1}. The peptide concentration ranges from 0.05 to 0.5 mg mL^{-1}. The fluorescence intensity at 468 nm (crystalline ellipticine) increases with time and reaches a plateau for all peptide concentrations used, but the time required to reach equilibrium is dependent on the peptide concentration (Fig. 4a). The equilibration time is at minimum (~5 h) when the peptide concentration is ~0.1 mg mL^{-1}, which is the reported critical aggregation concentration (CAC) of the peptide.[32] When the peptide concentration is away from the CAC, the equilibration time increases (>10 h). The change in the fluorescence intensity at 520 nm (protonated ellipticine) is also strongly dependent on the peptide concentration as shown in Figure 4b. Above the CAC, the protonated ellipticine can be seen to form and over time to disappear. The protonated ellipticine stays for a longer time (40 h) with a higher peptide concentration (0.5 mg mL^{-1}). At the CAC, the fluorescence of protonated ellipticine only appears in the first 2 h and quickly disappears afterwards. Below the CAC, no significant protonation of ellipticine is observed.

The overall equilibration time of the peptide-ellipticine complexation at different EAK16-II concentrations is listed in Table 1. The reported values were estimated from Figure 4, considering that both processes of ellipticine protonation and formation of stable ellipticine microcrystals have reached steady-state or equilibrium. Note that when the equilibrium of the both processes is reached, the final state of the stabilized ellipticine is mainly in crystalline form. It can be clearly seen that the overall equilibration time is strongly dependent on the peptide concentration and approaches a minimum when the peptide concentration is close to the CAC. This phenomenon may be related to the solution pH at various peptide concentrations and the peptide self-assembly.

At peptide concentrations below the CAC, the peptide solution has a relatively high pH, which prohibits ellipticine protonation. But under such a condition, microcrystals of ellipticine can form

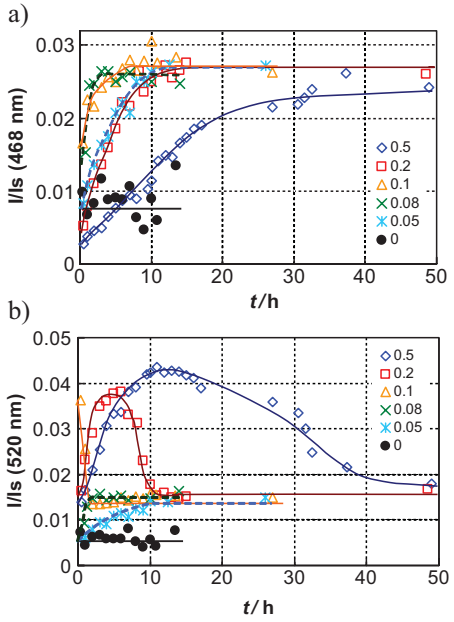

Figure 4. Effect of peptide concentration on the complex formation. The normalized fluorescence intensities of peptide-ellipticine suspensions as a function of time at 468 nm (a) and 520 nm (b). The ellipticine concentration was fixed at 1.0 mg mL^{-1} with various EAK16-II concentrations ranging from 0 to 0.5 mg mL^{-1}.

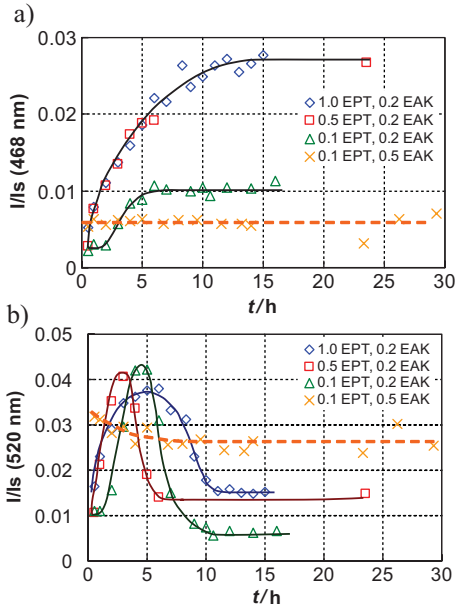

Figure 5. Effect of ellipticine concentration on the complex formation. The normalized fluorescence intensities of peptide-ellipticine suspensions as a function of time at 468 nm (a) and 520 nm (b). The 0.2 and 0.5 mg mL^{-1} EAK16-II were used with different ellipticine concentrations from 0.1 to 1.0 mg mL^{-1}.

over time. Such formation of ellipticine microcrystals becomes faster with increasing peptide concentration up to its CAC. At the CAC, a low pH, below the p*K*a of ellipticine, is observed. Such a low pH allows protonated ellipticine to form (Fig. 4b). However, over time peptide assemblies start to appear at this concentration; meanwhile the solution pH starts to increase and the number of available glutamic acid residues reduces. (Note that the glutamic acid residues can stabilize the protonated ellipticine.) As a result, deprotonation of ellipticine occurs shortly after the initial protonation.

At peptide concentrations above the CAC, a longer equilibration time is observed. This is probably due to the combined effects of the ellipticine protonation and microcrystal formation. The pH of a fresh peptide solution decreases with an increase in peptide concentration as shown in Table 1. At a concentration above the CAC, the solution has a pH below 5, which can induce the protonation of ellipticine. The lower the solution pH is, the more ellipticine can be protonated. The protonated ellipticine will gradually disappear with time while more stable ellipticine microcrystals form. It takes a longer time for protonated ellipticine to disappear at a higher peptide concentration, leading to a longer equilibration time.

Table 1. Peptide concentration-dependent equilibration time and solution pH.

[*EAK*] [mg mL^{-1}]	Estimated equilibration time [h] [a]	pH of fresh peptide solution [b]
0.50	40	3.9
0.20	15	4.6
0.10	7	5.2
0.08	4	5.5
0.05	12	6.0

[a] The equilibration time was estimated from Figure 3, considering that both I_{468} and I_{520} reach equilibrium. [b] The pH was measured from freshly prepared peptide solutions.

The peptide EAK16-II is capable of stabilizing ellipticine microcrystals and protonated ellipticine in aqueous solution in a time-dependent and peptide-concentration-dependent manner. The state of ellipticine could be critically important in its function as a therapeutic agent. It has been reported that the neutral form of ellipticine is active against various tumors.[26,33] Further in vitro and in vivo studies will elucidate the effects of the different states of ellipticine on its activity against cancer cells.

The ellipticine concentration effect on the complex formation was investigated with 0.2 mg mL^{-1} EAK16-II and three ellipticine concentrations: 1.0, 0.5, and 0.1 mg mL^{-1}. The change in fluorescence of crystalline and protonated ellipticine is shown in Figure 5a and b, respectively. At this peptide concentration, the ellipticine concentration does not seem to affect the overall equilibration time significantly. The time for the peptide-ellipticine suspension formation (both ellipticine protonation and formation of ellipticine microcrystals should reach equilibrium) is all ~10 h.

Interestingly, a particular combination of 0.1 mg mL^{-1} ellipticine with 0.5 mg mL^{-1} EAK16-II, increased from 0.2 mg mL^{-1}, can stabilize protonated ellipticine for a prolonged time (Fig. 5, crosses). The intensity at 520 nm decreases slightly at the beginning and reaches a plateau after 10 h, while that at 468 nm remains constant at a low value over time. The very low intensity at 468 nm is within the background noise, indicating that no ellipticine microcrystals can be detected. This result shows that

most ellipticine is protonated and solubilized in the solution. The slight initial decrease in intensity of the protonated ellipticine is likely the results of inner-filter effect as the solution solubilizes more ellipticine with time. The protonated ellipticine is stable for at least 50 h, the duration of the experiment, under continuous mechanical stirring. During this time period, the solution remains clear with a yellow-orange color. This particular combination of ellipticine and peptide concentrations suggests that a prolonged state of protonated ellipticine can be established. This will affect ellipticine release kinetics, and probably its therapeutic efficiency.

2.3. Release of Ellipticine from the Complex into EPC Vesicles

So far, we have shown the formation of peptide-ellipticine dispersions in water, either in microcrystal or protonated form. It is important to investigate how ellipticine releases from the peptide complex, and its release kinetics. This was done by mixing the complex with liposome vesicles, which mimic the cell membrane.[21]

Four peptide concentrations (0.05, 0.1, 0.2, and 0.5 mg mL^{-1}) were used to form peptide-ellipticine dispersions with 0.1 mg mL^{-1} of ellipticine in order to study the release kinetics. The samples were stirred for 24 h to ensure that equilibrium was reached. At 0.5 mg mL^{-1} of EAK16-II, the dispersion looks more yellow and less turbid comparing to others at lower peptide concentrations (see Supporting Information), providing the additional evidence to the results of Figure 5 that the 0.5 mg mL^{-1} EAK16-II solution can stabilize protonated ellipticine for a prolonged time. The different states of ellipticine at equilibrium can be clearly seen from their characteristic fluorescence spectra as shown in Figure 6. The suspension with 0.5 mg mL^{-1} EAK16-II has a pronounced peak located ~525 nm (protonated state) while those with peptide concentrations ranging from 0.05 to 0.2 mg mL^{-1} exhibit a peak of ~468 nm (crystalline state) (Fig. 6, inset). The very different properties of the complex suspensions according to the peptide concentration could also have significant effects on the ellipticine release (see below).

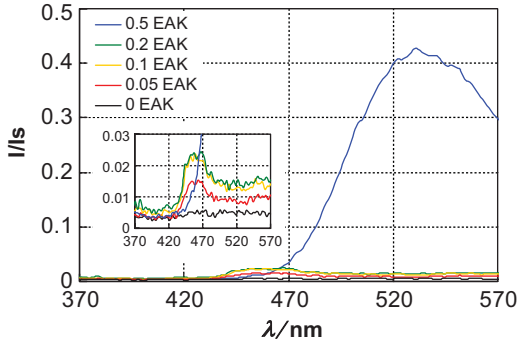

Figure 6. The fluorescence spectra of the peptide-ellipticine suspensions after 24 h stirring with 0.1 mg mL^{-1} ellipticine and various peptide concentrations of 0–0.5 mg mL^{-1}. Inset indicates the crystalline ellipticine fluorescence.

It is noted that the fluorescence of ellipticine, either protonated or in crystalline form upon interaction with peptides, is very different from that of ellipticine in EPC vesicles. Ellipticine in the vesicles exhibits a strong fluorescence signal at ~436 nm, which is characterized as neutral, monomeric ellipticine.[23] Such a signal can be well distinguished from those of the protonated ellipticine (~520 nm) and ellipticine crystals (weak fluorescence at ~468 nm). The transfer of ellipticine from the complex into the vesicles can be monitored by the change in ellipticine fluorescence at 436 nm over time

A typical transfer curve of ellipticine from the complex (0.05 mg mL^{-1} EAK16-II and 0.1 mg mL^{-1} ellipticine) to the EPC vesicles, or liposomes, is shown in Figure 7a. The fluorescence intensity at 436 nm increases with time and approaches to a plateau after 20 000 s. The reason that the initial point starts slightly above zero ($t = 0$) is probably due to the burst release of ellipticine into the vesicles during the initial sample mixing time (<30 s).

The transfer curve based on the ellipticine fluorescence can be related to its concentration accumulation in vesicles using a calibration curve (see Supporting Information). It was found that the vesicles were saturated with ellipticine when ellipticine concentration was above ~20 μM. Thus, the rising region in the calibration curve can be used to convert the fluorescence signals from the transfer profile to the ellipticine concentration in

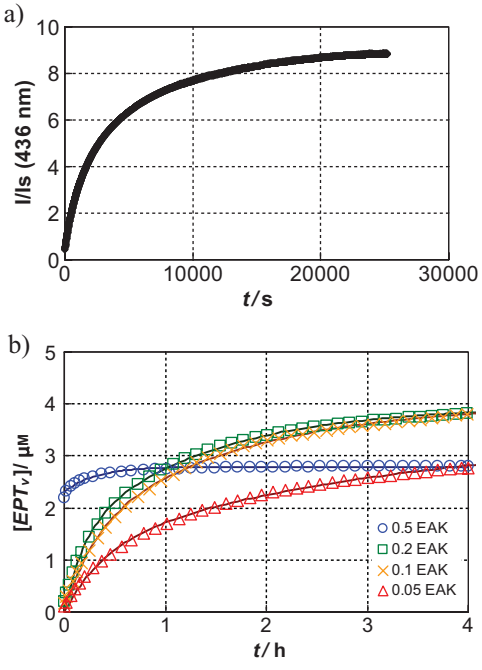

Figure 7. a) The time-dependent ellipticine fluorescence showing the release of ellipticine from the complex made of 0.05 mg mL^{-1} EAK16-II and 0.1 mg mL^{-1} ellipticine into the EPC vesicles. b) The transfer profiles of ellipticine from different peptide-ellipticine complexes to the EPC vesicles. The complexes were made of 0.1 mg mL^{-1} ellipticine with various EAK16-II concentrations: 0.05 (triangles), 0.1 (crosses), 0.2 (squares), and 0.5 mg mL^{-1} (circles). The solid lines represent the fitting curves to the data points using either Equation 2 or Equation 3. The excitation and emission wavelengths are 295 and 436 nm, respectively.

vesicles with a simple exponential equation:

$$I = A\left(1 - e^{-B[EPT]}\right) \quad (1)$$

The fitting parameters A and B are (17.5 ± 0.36) and $(230\,000 \pm 13\,400)$ M^{-1}, respectively. $[EPT]$ represents the concentration of ellipticine within the range of 0–20 μM. For a given fluorescence intensity of ellipticine ($I/I_s < 17.5$), one can obtain the corresponding ellipticine concentration using Equation 1.

Figure 7b shows four transfer profiles of ellipticine concentration in the vesicles ($[EPT_v]$) with time (h). Each curve corresponds to the transfer of ellipticine into the vesicles from different peptide-ellipticine complexes made with various EAK16-II concentrations. All profiles have a similar trend with a fast increase initially and gradually approaching a plateau. The very high initial values of the transfer profile from the complexes with 0.5 mg mL^{-1} EAK16-II indicate a burst release of ellipticine from the complex into the vesicles within 30 s. This is reasonable since the 0.5 mg mL^{-1} EAK16-II solution can stabilize protonated ellipticine (Figs. 5 and 6). These protonated ellipticine molecules may easily migrate into the lipid bilayers, causing a sudden increase in the ellipticine concentration in the vesicles. On the other hand, other peptide concentrations (0.05–0.2 mg mL^{-1}) do not stabilize protonated ellipticine but ellipticine microcrystals. The migration of ellipticine molecules from the microcrystals to the vesicles involves the molecularly dissolving of ellipticine, which is time consuming. Therefore, their transfer profiles do not have a large sudden increase, and start at values close to zero ellipticine concentration.

To better compare the transfer kinetics for the four different EAK16-II concentrations, the profiles were fitted to one of the following exponential equations. The second equation was used if the first could not satisfactorily describe the dynamics:[21]

$$[EPT_v](t) = [EPT_v]_{eq} - ([EPT_v]_{eq} - [EPT_v]_0)e^{-kt} \quad (2)$$

$$[EPT_v](t) = [EPT_v]_{eq}(1 - a_1 e^{-k_1 t} - a_2 e^{-k_2 t}) \quad (3)$$

where $[EPT_v](t)$, $[EPT_v]_{eq}$ and $[EPT_v]_0$ are the ellipticine concentration in the vesicles at time t, at equilibrium and at time zero, respectively; k, k_1, and k_2 are the rate constants; a_1 and a_2 are the pre-exponential factors and $a_1 + a_2 = 1$. The particular transfer profile with 0.5 mg mL^{-1} EAK16-II was fitted with Equation 2 where $[EPT_v]_0 \neq 0$ due to an initial burst transfer of ellipticine into the vesicles; the other three profiles were fitted well with Equation 3 as the initial transfer in these cases was very small and can be negligible. The rate constants are summarized in Table 2. Comparing the average rate constants for each transfer profile, it can be seen that the rate of transfer of ellipticine from the complexes into the vesicles increases with the peptide concentration during the preparation of peptide-ellipticine complexes.

This trend is opposite to that of our previous studies on the pyrene release from the EAK16-II coatings into the EPC vesicles.[21] The higher EAK16-II concentration used to form peptide-pyrene complexes results in a thicker coating on the pyrene microcrystals, which in turn causes a slower release rate.

Table 2. Transfer rates of ellipticine from peptide-ellipticine complexes to EPC liposomes.

[EAK]	0.5 mg mL^{-1} [a]	0.2 mg mL^{-1}	0.1 mg mL^{-1}	0.05 mg mL^{-1}
k_1 (h^{-1})	3.13 ± 0.14	5.20 ± 0.04	3.52 ± 0.03	2.53 ± 0.02
a_1		0.363 ± 0.002	0.345 ± 0.002	0.348 ± 0.003
k_2 (h^{-1})	n/a	0.75 ± 0.002	0.62 ± 0.002	0.30 ± 0.003
a_2		0.637 ± 0.002	0.655 ± 0.003	0.652 ± 0.002
k_{avg} [b]	3.13 ± 0.14	2.36 ± 0.02	1.62 ± 0.01	1.08 ± 0.01
R^2	0.976	0.999	0.999	0.999

[a] Denotes the fitting with Equation 2; all others with Equation 3. All the fitting parameters are significantly different from the statistical analysis. [b] $k_{avg} = a_1 k_1 + a_2 k_2$; $a_1 + a_2 = 1$.

In the present case of ellipticine, the higher peptide concentration induces the protonation of ellipticine and formation of smaller complexes as visualized by the SEM images in Figure 8. The size of the complexes with 0.5 mg mL^{-1} EAK16-II (Fig. 8a) is much smaller than that with 0.2 mg mL^{-1} EAK16-II (Fig. 8b). A further decrease in the peptide concentration (0.05 mg mL^{-1}) will result in a bigger size of the complexes as shown in Figure 8c. Since ellipticine in the vesicles is molecularly solubilized, the transfer process must involve the release of individual ellipticine molecules from the complexes; the bigger the complexes are, the longer the release of ellipticine from the complexes will be. Therefore, a slower transfer rate of ellipticine was observed at low peptide concentrations.

2.4. Cellular Toxicity of EAK16-II-Ellipticine Complexes

So far, we have shown that EAK16-II can stabilize ellipticine in protonated or crystalline form in aqueous solution, depending on the peptide and ellipticine concentrations. Protonated ellipticine can be stabilized in the complexes formulated with a combination of 0.5 mg mL^{-1} EAK16-II and 0.1 mg mL^{-1} ellipticine. When the ratio of peptide-to-ellipticine is smaller than 5:1 (by mass), the stabilized ellipticine is predominantly in crystalline form in the complexes (Fig. 5). This may indicate that the 5:1 ratio is important in determining the molecular states of ellipticine in the complexes. It is expected that the different molecular states will have different therapeutic effects against cancer cells.

Here a series of peptide-to-ellipticine ratios (at a fixed ellipticine concentration of 0.1 mg mL^{-1}) was used to form peptide-ellipticine complexes, and their cellular toxicity was investigated on two cancer cell lines, A549 and MCF-7, as shown in Figure 9a. The complexes at the ratios of 5:1 and 10:1 are effective at killing both cancer cells, leading to low cell viability (less than 0.25). Below the 5:1 ratio, the anticancer activity of the complexes decreases significantly, and is similar to the ellipticine control (no peptides). The dramatic change in the complex toxicity is probably related to the molecular state of ellipticine in the complexes. The protonated ellipticine appears to be more effective at killing cancer cells than crystalline ellipticine. This may be due to fast release kinetics of protonated ellipticine from the complexes (Fig. 7b). In addition, protonated ellipticine tends to interact with negatively charged cell membranes, and accumulate at the membrane surface; the hydrophobic moiety of ellipticine further helps it cross the cell membrane. This also

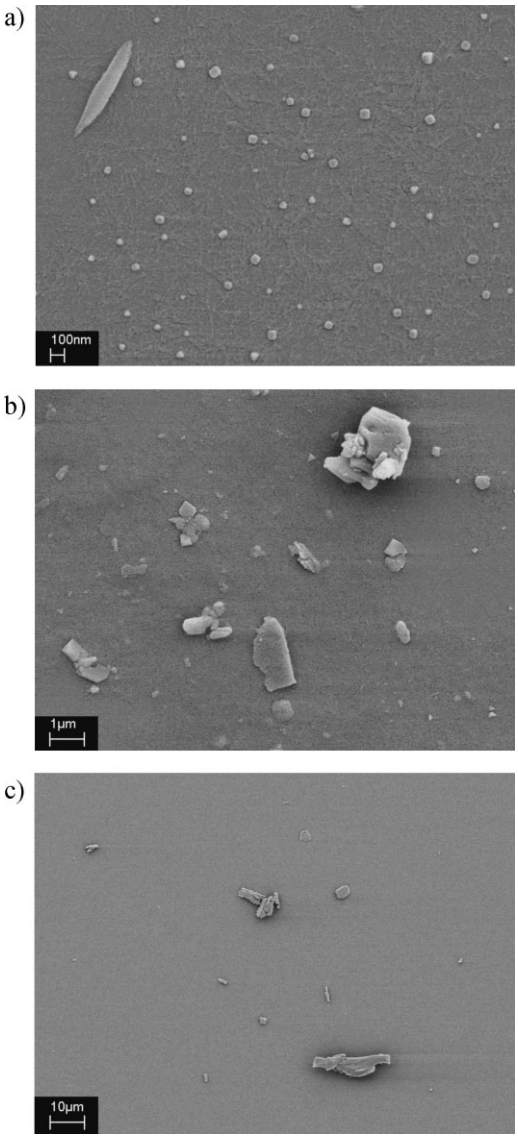

Figure 8. SEM images of the peptide-ellipticine complexes with 0.1 mg mL^{-1} ellipticine and different EAK16-II concentrations: a) 0.5 mg mL^{-1}, b) 0.2 mg mL^{-1}, and c) 0.05 mg mL^{-1}.

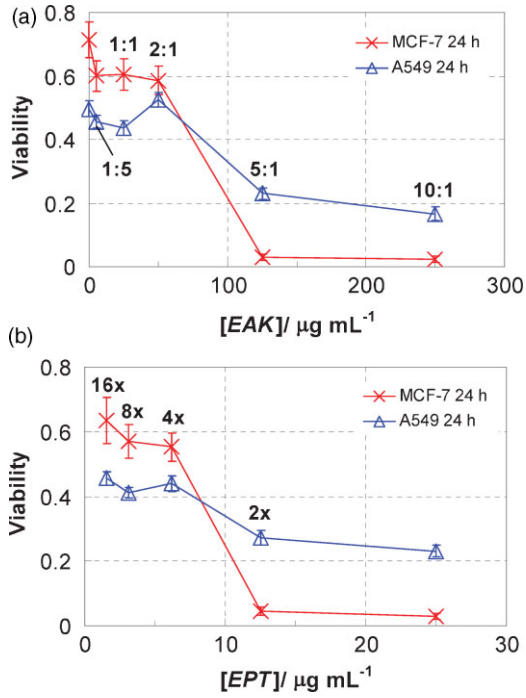

Figure 9. Viability of MCF-7 and A549 cells treated with the complexes for 24 h at different peptide-to-ellipticine ratios (a) and upon serial dilution (b). The complex at 5:1 ratio was used for the serial dilution. The complexes were prepared with a fixed ellipticine concentration of 0.1 mg mL^{-1} with various EAK16-II concentrations of 0.02–1.0 mg mL^{-1}.

implies that the internalization of ellipticine may not be through energy-dependent endocytosis.

Note that the protonated ellipticine seems to be more active at killing MCF-7 cells than A549 cells, causing an almost zero MCF-7 cell viability. Such an effect may be due to the fact that MCF-7, as cells are more sensitive to protonated ellipticine. Thus, these results may lead to a notion of selecting appropriate formulations to treat different cancer cells. By adjusting the mass ratio of EAK16-II versus ellipticine, one can obtain different molecular states of ellipticine in the complexes as well as the complex dimensions, for specific cancer cells.

The stability of a given formulation upon dilution is an important factor in determining its applicability in clinical usage.[34] Since the complexes at 5:1 ratio show a good anticancer activity against both cancer cell lines, we further carried out serial dilution of such complexes in pure water and test their stability in relation to the cellular toxicity. Figure 9b shows the toxicity of the complex prepared at a 5:1 ratio and its serial dilution in water (2, 4, 8, and 16 times). The 2 times dilution does not affect the toxicity of the complex significantly for both cells. Further dilution greatly reduces the complex toxicity against MCF-7 cells; it also decreases the toxicity against A549 cells, but to a lesser degree. Normally, the decrease in cell viability should be gradual and smooth due to the decrease in drug concentration upon dilution. However, the observed trend is not gradual, but rather a sharp change at more than 2x dilution. This may be related to the instability of the complexes upon dilution in water. One possible reason is that the complex containing protonated ellipticine is pH sensitive; extensive dilution is expected to increase the solution pH, leading to the deprotonation of ellipticine to form ellipticine microcrystals. As a result, the toxicity of the diluted complexes reduces, similar to that of the complexes prepared at a lower peptide-to-ellipticine ratio. Note that a drastic decrease in complex toxicity upon dilution for MCF-7 cells provides additional evidence that MCF-7 cells are more sensitive to protonated ellipticine.

The time-dependent toxicity of the complexes was further investigated and the results are shown in Figure 10. Two ratios, 1:1 (squares) and 5:1 (circles), were used to examine the difference in toxicity between crystalline and protonated ellipticine, respectively. They were compared with the ellipticine control (crosses) in the absence of EAK16-II. It can be seen that the two different cell lines exhibit different patterns in the time-dependent viability in response to the treatments. For MCF-7 cells

ADVANCED FUNCTIONAL MATERIALS

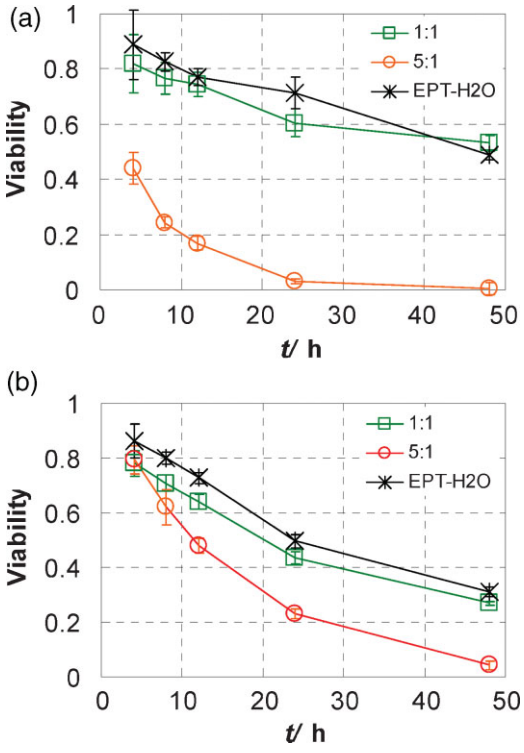

Figure 10. Time-dependent toxicity of the EAK16-II-ellipticine complexes against MCF-7 (a) and A549 (b) cells. EPT-H_2O: ellipticine control (in pure water).

(Fig. 10a), the complexes at the 5:1 ratio are so effective that the cell viability decreases to less than 0.5 after 4 h treatment; it decreases further to almost zero after 24 h treatment. Meanwhile, the complexes at the 1:1 ratio and ellipticine control have almost no effect at 4 h, before gradually decreasing the viability to about 0.5 by 48 h. On the other hand, no distinguishable difference in cell viability can be observed among the three treatments at 4 h for A549 cells (Fig. 10b); with time, all treatments cause significant cell death, although the effect is more pronounced for the complexes at 5:1 ratio. Almost zero viability is achieved after 48 h treatment with protonated ellipticine (5:1 ratio).

The above results indicate that again, MCF-7 cells are very sensitive to protonated ellipticine while both protonated and crystalline ellipticine are effective at killing A549 cells. However, the reason behind this is still unclear. One may speculate that such a phenomenon probably results from the differences in uptake of ellipticine in the complexes by A549 and MCF-7. Or it may be due to the different nature of the two cancer cell lines in response with ellipticine. Further experiments are required to study this phenomenon.

The study presented demonstrates that a self-assembling, ionic-complementary peptide, EAK16-II, can stabilize the hydrophobic anticancer agent ellipticine in aqueous solution. Different combinations of peptide and ellipticine concentrations can stabilize either protonated or crystalline ellipticine for an extended time. The ellipticine can be released from the complexes into a cell membrane mimic. The release rate is related to the peptide concentration used in the complexation. By optimizing the process of complex formation, one could obtain desired complex dimensions and drug release property. These factors and molecular states of ellipticine can have significant impacts on the cellular toxicity of the peptide-ellipticine complexes.

The results obtained here will be important in the next phase studies on the peptide-based delivery of ellipticine in vivo. First, the size of the peptide-ellipticine complexes can be controlled from micrometers to hundreds of nanometers. The particle size will significantly affect the circulation in the blood stream, binding to the cells and uptake by the cells.[35–38] The size of the complexes ranging from 100 nm to 500 nm would be ideal for passive targeting to solid tumors via the enhanced permeability and retention (EPR) effect.[6,39–41] Second, different molecular states of stabilized ellipticine in solution can be obtained depending on peptide and ellipticine concentrations used in the formulation. This will have a varying impact on the anticancer activity and therapeutic efficacy.[42–44] Current results demonstrate that the complexes with protonated ellipticine are more effective at killing MCF-7 cells in vitro. Third, the release rate of ellipticine from the complex can be tuned, in relation to the size of the complex and the molecular state of stabilized ellipticine. The in vivo animal studies are currently undergoing.

3. Conclusions

The ionic-complementary self-assembling peptide EAK16-II was found to be able to stabilize the hydrophobic anticancer agent ellipticine in aqueous solution. Both microcrystal and protonated forms of ellipticine can be obtained in the complexes. The complex formation in water is peptide concentration-dependent. When the peptide concentration was close to its CAC (~0.1 mg mL^{-1}), the equilibration time for complex formation could be as short as 5 h. At higher and lower peptide concentrations, the time required to reach equilibrium became much longer. High peptide concentrations facilitated the formation of protonated ellipticine during the complexation while low peptide concentrations favored crystalline ellipticine formation. With a combination of 0.1 mg mL^{-1} ellipticine and 0.5 mg mL^{-1} EAK16-II, protonated ellipticine can be stabilized. The transfer rate of ellipticine from its peptide complexes into EPC vesicles was dependent on the peptide concentration used during the peptide-ellipticine formulation. A higher peptide concentration resulted in a faster release rate, relating to the fact that higher peptide concentrations favor protonation of ellipticine and formation of smaller complexes. In addition, the size of the EAK16-II-ellipticine complex could be tuned by adjusting the peptide-to-ellipticine ratio (by mass) during formulation. The cellular toxicity results indicated that the complexes (≥5:1 ratio) with protonated ellipticine were effective at killing both MCF-7 and A549 cells, although their stability upon dilution in water was not very good. This study demonstrates the capability of ionic-complementary, self-assembling peptides as carriers for hydrophobic anticancer drug delivery.

4. Experimental

Materials: The peptide EAK16-II (M_w = 1657 g mol^{-1}, crude) was purchased from CanPeptide Inc. (Montreal, Canada) and used without

further purification. It has a sequence of AEAEAKAKAEAEAKAK (Fig. 1), where A corresponds to alanine, E to glutamic acid and K to lysine. The N-terminus and C-terminus of the peptide were protected by acetyl and amino groups, respectively. The anticancer agent ellipticine (99.8% pure) was purchased from Sigma–Aldrich (Oakville, Canada) and used as received. Egg Phosphatidylcholine (EPC, powder, >99% pure) was obtained from Avanti Polar Lipids, Inc. (Alabaster, AL). Ethylenediaminetetraacetic acid (EDTA) was from Bio-Rad Laboratories (Mississauga, Canada). Tris(hydroxymethyl)methylamine (Tris) and glacial acetic acid were bought from BDH Inc. (Toronto, Canada). Cell culture reagents, including Dulbecco's modified eagle medium (DMEM), fetal bovine serum (FBS) and trypsin-ETDA, were purchased from Invitrogen Canada Inc. (Burlington, ON, Canada). Phosphate buffer saline (PBS) and penicillin-streptomycin (p/s, 10000 U) were obtained from MP Biomedicals Inc. (Solon, OH, USA).

Liposome Preparation: EPC powders (~5 g) were weighed and dissolved in a buffer solution (125 mL) containing Tris/acetic acid (25 mM, pH = 7.0) and EDTA (0.2 mM). The mixture was then extruded using a LiposoFast-Basic extruder (Avestin Inc., Ottawa, Canada) with a polycarbonate membrane (100 nm pore size) to obtain uniform liposome dispersions at room temperature. The dispersions were further diluted (4×) with the same Tris/acetic acid buffer. This was followed by centrifugation at 4 000 rpm for 1 h to eliminate the larger vesicles and possible contaminates. The supernatant was collected and stored at 4 °C before use. The EPC concentration was determined to be 7.1×10^{-4} M using the method described in our previous publication [21]. The size of the EPC liposomes was characterized by a Dynamic Light Scattering (DLS) technique; their hydrodynamic diameter (intensity-based) was found to be around 200 nm (see Supporting Information).

Formation of Peptide-Ellipticine Complexes: To make peptide-ellipticine complexes, certain amounts of ellipticine crystals were added into fresh EAK16-II solutions (0.02–1.0 mg mL^{-1}) to have ellipticine concentrations of 0.1–1.0 mg mL^{-1}. The fresh peptide solutions were prepared by dissolving peptide powder in pure water (18.2 MΩ, Milli-Q A10 synthesis), followed by sonication for 10 min. The peptide-ellipticine mixtures were stirred at 900 rpm on a magnetic stir plate throughout the complexation experiment. At specified times, the mixtures were transferred to a quartz cuvette to acquire fluorescence spectra of ellipticine on a steady-state spectrofluorometer (Photon Technology International, London, Canada). The test was performed once every hour for the first 20 h and less frequently for the remaining period until an equilibrium state was reached. Ellipticine (1 mg mL^{-1}) in pure water was prepared as a control.

Since the peptide can self-assemble over time, it is expected that a competition may exist between the peptide-peptide association and the peptide-ellipticine complexation during the drug formulation. To better understand such a complicated process, the peptide assembly without ellipticine was investigated. For this purpose, fresh EAK16-II solution (0.2 mg mL^{-1}) was prepared and stirred for 30 h at 900 rpm. The peptide assembly was characterized by static light scattering (at 400 nm) acquired on the steady-state spectrofluorometer and compared with the fresh peptide solution (0 h). The light scattering intensity of air was obtained as the standard to correct for the lamp fluctuations.

For the ellipticine release experiments, the complexes were newly prepared with a fixed ellipticine concentration of 0.1 mg mL^{-1} and various peptide concentrations ranging from 0.05 to 0.5 mg mL^{-1}. The samples were continuously stirred for 24 h to ensure that equilibrium was reached in the mixture. The steady-state fluorescence spectra of the complexes were acquired just before the release experiments (to show the states of ellipticine in complexes different from that in EPC vesicles).

For cellular toxicity tests, the complexes were prepared with 0.1 mg mL^{-1} ellipticine and fresh EAK16-II solutions at concentrations of 0.02, 0.1, 0.2, 0.5, and 1.0 mg ml^{-1}, generating five peptide-to-ellipticine ratios of 1:5, 1:1, 2:1, 5:1, and 10:1 (by mass), respectively. The EAK16-II-ellipticine mixtures were under mechanical stirring at 900 rpm for 24 h. An ellipticine control in pure water (with the absence of EAK16-II) at the same ellipticine concentration was prepared for comparison, following the same procedure. The complexes at a 5:1 ratio were diluted serially (2×, 4×, 8× and 16×) in pure water to study the complex stability. All vials and solvents were sterilized and the samples were prepared in a biological safety cabinet to avoid possible contamination. The appearance of the peptide-ellipticine suspensions was recorded in conjunction with the ellipticine fluorescence spectra, to determine the different molecular states of ellipticine in the complexes.

Ellipticine Release into Liposome Vesicles: The release of ellipticine from the complex into the EPC vesicles was continuously monitored on the spectrofluorometer over time. The experiments were conducted with the following procedure: the peptide-ellipticine dispersion (100 μL) were transferred into a quartz cuvette and mixed with EPC vesicles (2.9 mL). The 30 times dilution of the complex upon mixing with the vesicles was to ensure that the final ellipticine concentration was in the range where the calibration curve was applicable. The cuvette was then put in the spectrofluorometer with gentle magnetic stirring, covered with a parafilm on top (to eliminate the water evaporation during the course of measurement) before starting to collect the fluorescence over time. The time required to prepare the sample before starting a time-dependent fluorescence measurement was less than 30 s.

Steady-State Fluorescence Measurements: The ellipticine fluorescence was acquired on a Photon Technology International spectrafluorometer (Type QM4-SE, London, Canada) with a continuous xenon lamp as the light source. For each sample, solutions (~3 mL) were transferred from a vial into a square quartz cell (1 cm × 1 cm) through a Pasteur glass pipette. All samples containing ellipticine were excited at 294 nm and the emission spectra were collected from 320 to 650 nm. The excitation and emission slit widths were set at 0.25 mm and 0.5 mm, respectively (0.25 mm corresponds to 1-nm band path). The fluorescence intensity at 468 nm and 520 nm were obtained by taking the average from 458 to 478 nm and 510 to 530 nm, respectively. A standard (2 μM ellipticine in ethanol, sealed and degassed) was used in each run to correct the lamp intensity variations. The standard fluorescence intensity I_s was obtained by taking the average of the fluorescence from 424 to 432 nm (peak at ~428 nm). The kinetics of the ellipticine release from the complex into the EPC vesicles was monitored by acquiring the time-dependent ellipticine fluorescence at 436 nm over a 7 h time span at 5 s intervals. All solutions reached equilibrium within 7 h as the fluorescence intensities reached a plateau during the experimental time span. The same standard sample as described above was used to obtain I_s (at 428 nm over 10 min) to correct for the day-to-day fluctuations. For each release experiment, the fluorescence was recorded while the solution was gently stirred in the spectrafluorometer.

SEM: A LEO model 1530 field emission SEM (GmbH, Oberkochen, Germany) was employed to study the morphology and dimensions of the peptide-ellipticine complex. The SEM samples were prepared by depositing the complex suspensions (20 μL) on a freshly cleaved mica surface. The mica was affixed on an SEM stub using a conductive carbon tape. The sample was placed under a Petridish-cover for 10 min to allow the complexes adhering to the mica surface. It was then washed once with pure water (100 μL) and air-dried in a desicator overnight. All samples were coated with a 20 nm thick gold layer prior to imaging; the images were acquired using the secondary electron (SE2) mode at 5 kV.

Cellular Toxicity Tests: Two cancer cell lines, non-small cell lung cancer cell A549 and breast cancer cell MCF-7, were used for in vitro cellular toxicity studies on the EAK16-II-ellipticine complexes. The cells were cultured in DMEM containing 10% FBS and 1% p/s at 37 °C and with 5% CO_2. When the cells grew to reach ~95% confluence, they were detached from the cell culture dishes with trypsin-EDTA, centrifuged at 500 rpm for 5 min, and resuspended in fresh cell culture media at concentrations of 5×10^4 and 1×10^5 cells mL^{-1} for A549 and MCF-7 cells, respectively. For each type of cell, the cell suspensions (200 μL) were added into each well of a clear, flat bottom, 96-well plate (Costar) and incubated for ~24 h. The old media were taken out and replaced with fresh culture media (150 μL), followed by an addition of treatments (50 μL, including the complexes and control samples) into each well, resulting in a 4-fold dilution of the treatments. The plates were incubated for 4, 8, 12, 24, and 48 h prior to performing the cell viability assay. The experimental setup contained

several control groups for each plate, including negative control (medium), solvent control, peptide control and drug control.

MTT assay (TOX1 from Sigma–Aldrich, Oakville, ON, Canada) was used to determine the cell viability after each treatment. Solid MTT (5 mg) was first dissolved in PBS solution (3 mL), followed by a 10-time dilution in the culture medium. All the treatments were taken out, and the MTT solution (100 μL) was then added to each well of the treated plates. The plates were incubated for 4 h prior to the addition of solubilization solution (100 μL, anhydrous isopropanol with 0.1 N HCl and 10% Triton X-100). After overnight incubation, the absorbance at 570 nm was collected on a microplate reader (BMG FLUOstar OPTIMA) and subtracted by the background signals at 690 nm. The absorption intensities were averaged from 4 replicates for each treatment and normalized to that obtained from the untreated cells (negative control) to generate the cell viability (i.e., the cell viability of the negative control is 1).

Acknowledgements

This research was financially supported by the Natural Sciences and Engineering Research Council of Canada (NSERC), Canadian Foundation for Innovation (CFI), the Canadian Institutes of Health Research (CIHR), the Canada Research Chairs (CRC) Program to one of the co-authors (PC) and the Canada Graduate Scholarships (CGS) Program to one of the co-authors (SYF). We also thank Dr. Jean Duhamel for the helpful discussion on our early experiments of the complex formation, Dr. Bing Han and Peter Tang for initial cell culture experiments, and Hui Wang for some fluorescence experiments. Supporting Information is available online from Wiley InterScience or from the authors.

Received: June 27, 2008
Published online: December 4, 2008

[1] J. Kopecek, *Eur. J. Pharm. Sci.* **2003**, *20*, 1.
[2] V. P. Torchilin, *Curr. Drug Delivery* **2005**, *2*, 319.
[3] J. J. Schwartz, S. Zhang, *Curr. Opin. Mol. Ther.* **2000**, *2*, 162.
[4] J. Hawiger, *Curr. Opin. Chem. Biol.* **1999**, *3*, 89.
[5] O. H. Aina, T. C. Sroka, M.-L. Chen, K. S. Lam, *Biopolymers* **2002**, *66*, 184.
[6] F. X. Gu, R. Karnik, A. Z. Wang, F. Alexis, E. Levy-Nissenbaum, S. Hong, R. S. Langer, O. C. Farokhzad, *Nanotoday* **2007**, *2*, 14.
[7] R. Langer, *Nature* **1998**, *392*, 5.
[8] C. B. Carlson, P. Mowery, R. M. Owen, E. C. Dykhuizen, L. L. Kiessling, *ACS Chem. Biol.* **2007**, *2*, 119.
[9] D. Derossi, G. Chassaing, A. Prochiantz, *Trends Cell Biol.* **1998**, *8*, 84.
[10] M. Lindgren, M. Hallbrink, A. Prochiantz, U. Langel, *Trends Pharmacol. Sci.* **2000**, *21*, 99.
[11] P. Lundberg, U. Langel, *J. Mol. Recognit.* **2003**, *16*, 227.
[12] J. Temsamani, P. Vidal, *Drug Discovery Today* **2004**, *9*, 1012.
[13] O. H. Aina, T. C. Sroka, M.-L. Chen, K. S. Lam, *Biopolymers* **2002**, *66*, 184.
[14] J. Oehlke, B. Wiesner, M. Bienert, in *Handbook of Cell-Penetrating Peptides,* (Ed. U. Langel), CRC Press LLC, Boca Raton, FL **2002**, pp. 71–92.
[15] S. Y. Fung, Y. Hong, C. Keyes-Baig, P. Chen, in *Molecular Interfacial Phenomena of Polymers and Biopolymers*, (Ed: P. Chen), Woodhead Publishing Ltd., Cambridge, England **2005**, pp. 421–474.
[16] P. C. H. Hsieh, M. E. Davis, J. Gannon, C. MacGillivray, R. T. Lee, *J. Clin. Invest.* **2006**, *116*, 237.
[17] M. E. Davis, P. C. H. Hsieh, T. Takahashi, Q. Song, S. Zhang, R. D. Kamm, A. J. Grodzinsky, P. Anversa, R. T. Lee, *Proc. Natl. Acad. Sci. USA* **2006**, *103*, 8155.
[18] T. C. Holmes, S. de Lacalle, X. Su, G. Liu, A. Rich, S. Zhang, *Proc. Natl. Acad. Sci. USA* **2000**, *97*, 6728.
[19] S. Zhang, T. Holmes, C. Lockshin, A. Rich, *Proc. Natl. Acad. Sci. USA* **1993**, *90*, 3334.
[20] S. Zhang, T. Holmes, C. M. DiPersio, R. O. Hynes, X. Su, A. Rich, *Biomaterials* **1995**, *16*, 1385.
[21] C. Keyes-Baig, J. Duhamel, S. Y. Fung, J. Bezaire, P. Chen, *J. Am. Chem. Soc.* **2004**, *126*, 7522.
[22] S. Y. Fung, H. Yang, P. Chen, *Colloids Surf. B* **2007**, *55*, 200.
[23] S. Y. Fung, J. Duhamel, P. Chen, *J. Phys. Chem. A* **2006**, *110*, 11446.
[24] J. Liu, Y. Xiao, C. Allen, *J. Pharm. Sci.* **2004**, *93*, 132.
[25] J. Duhamel, in *Molecular Interfacial Phenomena of Polymers and Biopolymers*, (Ed: P. Chen), Woodhead Publishing Ltd., Cambridge, England **2005**, pp. 214–248.
[26] N. C. Garbett, D. E. Graves, *Curr. Med. Chem.: Anti-Cancer Agents* **2004**, *4*, 149.
[27] A. Clarysse, A. Brugarolas, P. Siegenthaler, R. Abele, F. Cavalli, R. de Jager, G. Renard, M. Rozencweig, H. H. Hansen, *Eur. J. Cancer Clin. Oncol.* **1984**, *20*, 243.
[28] M. Sbai, S. Ait Lyazidi, D. A. Lerner, B. del Castillo, M. A. Martin, *J. Pharm. Biomed. Anal.* **1996**, *14*, 959.
[29] J. M. El Hage Chahine, J.-P. Bertigny, M.-A. Schwaller, *J. Chem. Soc. Perkin Trans. 2* **1989**, 629.
[30] H. Yang, S. Y. Fung, M. D. Pritzker, P. Chen, *J. Am. Chem. Soc.* **2007**, *129*, 12200.
[31] H. Yang, S. Y. Fung, M. D. Pritzker, P. Chen, *PLoS One* **2007**, *2*, e1325.
[32] S. Y. Fung, C. Keyes, J. Duhamel, P. Chen, *Biophys. J.* **2003**, *85*, 537.
[33] M. Sainsbury, in *The Chemistry of Antitumour Agents*, (Ed: D. E. V. Wilman), Chapman and Hall, New York, NY **1990**, pp. 411–435.
[34] J. L. S. Au, S. H. Jang, M. G. Wientjes, *J. Controlled Release* **2002**, *78*, 81.
[35] C. Cortez, E. Tomaskovic-Crook, A. P. R. Johnston, A. M. Scott, E. C. Nice, J. K. Heath, F. Caruso, *ACS Nano* **2007**, *1*, 93.
[36] G. Kong, R. D. Braun, M. W. Dewhirst, *Cancer Res.* **2000**, *60*, 4440.
[37] W. Zauner, N. A. Farrow, A. M. R. Haines, *J. Controlled Release* **2001**, *71*, 39.
[38] K. Y. Win, S.-S. Feng, *Biomaterials* **2005**, *26*, 2713.
[39] I. Brigger, C. Dubernet, P. Couvreur, *Adv. Drug Delivery Rev.* **2002**, *54*, 631.
[40] K. Greish, *J. Drug Targeting* **2007**, *15*, 457.
[41] H. Maeda, T. Sawa, T. Konno, *J. Controlled Release* **2001**, *74*, 47.
[42] X. Li, D. J. Hirsh, D. Cabral-Lilly, A. Zirkel, S. M. Gruner, A. S. Jano, W. R. Perkins, *Biochim. Biophys. Acta* **1998**, *1415*, 23.
[43] R. Garcia-Carbonero, J. G. Supko, *Clin. Cancer Res.* **2002**, *8*, 641.
[44] A. Hatefi, B. Amsden, *Pharm. Res.* **2002**, *19*, 1389.